ARTICLES

Journal of Semiconductors
(2019) 40, 022101
doi: 10.1088/1674-4926/40/2/022101

Three-dimensional hierarchical CuO gas sensor modified by Au nanoparticles

Qi Lei[1], Hairong Li[1, 2, 3, †], Huan Zhang[1], Jianan Wang[1], Wenhao Fan[1], and Lina Cai[1]

[1]School of Physical Science and Technology, Lanzhou University, Lanzhou 730000, China

[2]Key Laboratory of Special Function Materials and Structure Design, Ministry of Education, Lanzhou University, Lanzhou 730000, China

[3]Institute of Sensor Technology, Gansu Academy of Sciences, Lanzhou 730000, China

Abstract: The three-dimensional hierarchical CuO and Au nanoparticles were synthesized by the hydrothermal method, respectively. The hierarchical CuO and the Au nanoparticles samples were characterized by X-ray diffraction and scanning electronic microscope, respectively. The as-synthesized CuO was assembled regularly from the nanosheets with thickness of 100 nm. The size of Au nanoparticles ranged from 50 to 200 nm. The hierarchical CuO gas sensors modified by different concentration of gold were fabricated. All the Au-loaded CuO gas sensors enhanced the response to ethanol and xylene while reducing the response to methanol, acetone, and formaldehyde. The results indicate that the Au nanoparticles prepared with PVP as surfactant can improve the selectivity of CuO gas sensors to ethanol gas for other common organic volatile gases. The improvement of gas sensing is mainly attributed to the different catalytic efficiency of the Au nanoparticles for different reactions. Meanwhile, the related mechanisms are discussed.

Key words: CuO; Au nanoparticle; gas sensor; selectivity

Citation: Q Lei, H R Li, H Zhang, J N Wang, W H Fan, and L N Cai, Three-dimensional hierarchical CuO gas sensor modified by Au nanoparticles[J]. *J. Semicond.*, 2019, 40(2), 022101. http://doi.org/10.1088/1674-4926/40/2/022101

1. Introduction

Since the gas sensitivity of the material was discovered, it has been widely concerned in the field of gas detection. The gas sensors have been widely used, including the detection of industrial toxic or explosive gases[1], the measurement of indoor harmful gases[2, 3], environmental monitoring[4], medical and food fields[5, 6], etc. At present, many types of gas sensors have been developed, such as semiconductor gas sensors, contact combustion gas sensors, and electrochemical gas sensors[7–9]. Metal oxide semiconductors are widely used in gas sensors due to their outstanding gas sensitivity and being easy to synthesize[10–16]. ZnO, SnO_2, Fe_2O_3, TiO_2, and In_2O_3, etc. are N-type metal oxide semiconductors commonly used for gas sensors. CuO, NiO, and Co_3O_4, etc. are typical P-type metal oxide semiconductors. However, the N-type metal oxide semiconductors generally have wide band gap and high resistance. For example, the band gap of SnO_2 is about 3.6 eV. The initial resistance of the SnO_2 gas sensors fabricated by Dong *et al.*[17] was as high as 11 MΩ. The high value of resistance will increase the design difficulty and the cost of the test circuit. CuO (~1.2 eV) as a P-type metal oxide semiconductor with a narrow band gap usually has a smaller resistance. The initial resistance of the CuO gas sensors fabricated by our previous work[18] was about 20 kΩ. Therefore, CuO as the P-type semiconductor gas sensors have obvious advantages of application. However, there are few researches on the CuO gas sensors compared with the N-type metal oxide semiconductors gas sensors. In the past few decades, a lot of research has been done to improve the performance of gas sensors. For example, different morphologies of the CuO were synthesized for increasing the specific surface area of the material[19, 20]. The oxide-based heterojunctions materials were discussed in depth[21]. Various metals or metallic oxides were used to modify gas sensitive materials[22–27]. Particularly, noble metal decoration on the surface of metal oxides usually showed enhanced sensing properties evidently compared to pristine materials[28–30]. These researches have effectively improved the response of materials to target gases. However, few researches have been done on improving the selectivity of the gas sensors for the common organic volatile gases (ethanol, methanol, acetone, formaldehyde, xylene, etc.). As we know, it is very important to detect and identify a target gas accurately in a laboratory or industrial workshop filled with organic volatile gases. So, it is an urgent problem. So far, there have been no theories of guiding for the selectivity of gas sensors, except for a few kinds of special gases like H_2S[31]. Although some mechanisms have described the reaction of organic volatile gases with adsorbed oxygen ions on the surface of the material[32, 33], these have little practical significance in improving the gas selectivity. Without the support of relevant theories, the design of the experimental schemes to improve the selectivity of gas sensors is rather difficult. In previous researches, the response of all test gases was improved while improving the performance of gas sensors. This usually had little effect on improving the selectivity of gas sensors. However, if a method can reduce the response or increase the response weakly to other gases while obviously increase the response to a kind of target gas. It will improve the selectivity of this gas to a certain extent. Considering that the catalysts have different catalytic efficiencies for different reactions, we researched the effect of Au nanoparticles on the selectivity of nano-CuO gas sensors using Au nanoparticles as

Correspondence to: H R Li, lzulihairong@163.com
Received 11 JULY 2018; Revised 21 AUGUST 2018.

catalysts.

Herein, we synthesized three-dimensional (3D) CuO nanomaterials assembled from nanosheets. Meanwhile, Au nanoparticles were synthesized and the method was similar to the preparation of Ag nanoparticles[34]. The Au-loaded CuO gas sensors were fabricated and used to detect common volatile organic compounds ethanol, methanol, acetone, formaldehyde, and xylene. Through the loading of gold nanoparticles, the response of gas sensors to ethanol and xylene had been improved while reducing the response to 400 ppm of methanol, acetone, and formaldehyde to 61%, 66%, and 58%, respectively, at the optimum operating temperature (about 160 °C). It led to the response toward ethanol being significantly higher than the response to other gases, and the selectivity of the gas sensors for ethanol was effectively improved. The phase structure and the morphology were also researched to give a further understanding of the relevant mechanism.

2. Experimental section

2.1. Synthesis process

2.1.1. Preparation of CuO nanomaterial

All the chemical regents (analytical grade) were directly used without further purification. CuO nanomaterials are synthesized by the hydrothermal method, which is similar to the method of Yang and Liu[35]. In a typical process, 2.4 g of $Cu(NO_3)_2{\cdot}3H_2O$ was dissolved in 10 mL of deionized water, and 0.2 g of NaOH was dissolved in 5 mL of deionized water. Then the NaOH solution was added dropwise to the $Cu(NO_3)_2$ solution with vigorous stirring. Later, 0.6 g $C_6H_{12}N_4$ was added to the blue turbid liquid, and 20 mL of deionized water was added after stirring for 5 min. 35 mL of the suspension was transferred into a 50 mL of Teflon-lined stainless steel autoclave, and continuously heated at 120 °C for 15 h. Then it was naturally cooled to room temperature. The precipitate was collected by centrifugation and washed 3 times with deionized water and ethanol alternately, then dried in a vacuum at 90 °C for 6 h. Finally, the black powder was calcined at 500 °C for 2 h with a heating rate of 5 °C/min.

2.1.2. Preparation of Au-loaded CuO nanomaterial

For the synthesis of Au nanoparticles, 4.0 g glucose and 0.9 g PVP (K30) were dissolved into 30 mL deionized water, and 4.1 mL $HAuCl_4$ solution (0.02 M) was added dropwise into the above solution under vigorous stirring. Then the above solution was transferred into a 50 mL of Teflon-lined stainless steel autoclave, and continuously heated at 180 °C for 4 h. After the autoclave was quickly cooled by cold water, nano-gold nanoparticles were collected and washed twice with deionized water and ethanol alternately by centrifugation at 9000 rpm. Finally, the Au nanoparticles were dispersed in ethanol with the assistance of ultrasonication.

The CuO powder and Au nanoparticles were dispersed into Ethanol solvent, and the samples were prepared through adjusting the molar ratio of Au to CuO. The obtained product was named pure CuO: 0.5 Au–CuO, 1.0 Au–CuO, and 2.0 Au–CuO (corresponding to the ratio 0, 0.5‰, 1.0‰, and 2.0‰, respectively.)

2.2. Characterization

The as-synthesized CuO nanomaterial and Au nanoparticles were characterized by X-ray diffraction (XRD, Rigaku D/max-2400) with copper Kα radiation. The microscopic images of the products were obtained by scanning electron microscopy (SEM, Hitachi S-4800).

2.3. Fabrication and measurement of gas sensors

The gas sensor was fabricated using ceramic tube adjacent thermal structure in accordance with literature[18]. The hollow ceramic tube has a pair of gold electrodes at both ends, and two platinum wires are connected to each gold electrode as the test electrodes. A Ni–Cr heating wire (about 30 Ω) is inserted into the hollow ceramic tube to heat the device to control the operating temperature. First, the samples dispersed in ethanol were transferred to the surface of ceramic tubes, and uniformly covered on the surface of the ceramic tube to guarantee good contact with the gold electrode. Then, the device was aged at 200 °C for 24 h in air to improve the stability. Finally, the gas sensing characteristics of the gas sensing device were measured using a QJC-II system. During the testing process, when the initial resistance of the gas sensor was stable in a test chamber, the target volatile liquid is injected into the chamber (35.138 L) with a micro injector. Then, the liquid was volatilized by the fast evaporator and mixed evenly in the chamber. Next, the resistance of the gas sensor gradually became stable after changing, and the gas sensor was exposed to the air. The resistance of the gas sensors in the air was defined as R_a, and the resistance of the gas sensors in the target gas was defined as R_g, and the gas response was defined as Eq. (1):

$$S = R_g/R_a. \tag{1}$$

The response time (T_{res}) and recovery time (T_{rec}) were defined as the time required for the resistance to reach 90% of the final equilibrium value in the case of adsorption and desorption, respectively. The concentration of the target gas in the chamber was calculated by Eq. (2):

$$C = 24.5\rho V_1\varphi/(MV_2)\times 10^6, \tag{2}$$

where C (ppm) is the target gas concentration in the chamber, 24.5 is the gas molar volume at 25 °C 101 kPa, ρ (g/mL) is the density of volatile liquid, V_1 (μL) is the volume of volatile liquid, φ is the actual content of the target substance in the liquid, M (g/mol) is the molar mass of the target substance, and V_2 (L) is the volume of the chamber.

3. Results and discussion

3.1. X-ray diffraction and morphology analysis

The material composition and phase structure of the samples were determined by XRD. Fig. 1(a) shows the XRD pattern of the as-synthesized Au nanoparticles, all diffraction peaks were matched with JCPDS 04-0784 of Au. The peak of angle 20° to 30° was the amorphous diffraction peak of glass substrate. The peaks centered at 38.18°, 44.39°, and 64.58° were indexed to the (111), (200), and (220) planes of Au, respectively. The sample was identified as the Au. Fig. 1(b) shows the XRD pattern of the as-synthesized Au–CuO and pure CuO nanomaterials, all diffraction peaks were matched with JCPDS 48-1548 of CuO for the pure CuO samples. Such as the diffraction peaks of the as-synthesized CuO nanomaterial at 2θ 35.54°, 38.71°, 48.72°, and 61.52° were indexed to the $(11\bar{1})$, (111), $(20\bar{2})$, and $(11\bar{3})$ planes, respectively. The sample was identified as CuO. The XRD pattern of the Au-loaded CuO nanomaterials was also provided. The peak of the Au nanoparticles of the (111) plane coincided with the diffraction peak of the (111)

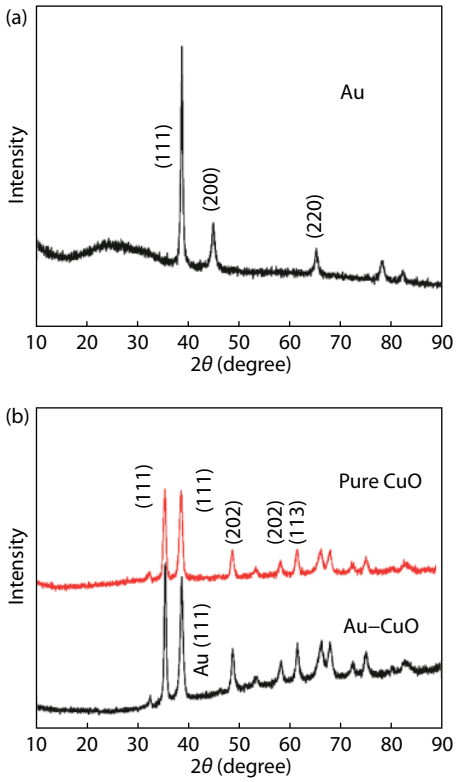

Fig. 1. (Color online) XRD patterns of (a) the Au samples, and (b) the Au–CuO and pure CuO samples.

plane of the CuO, while the other diffraction peaks of gold were not observed, because the concentration of gold was too low.

The morphologies of the as-synthesized CuO nanomaterial and Au nanoparticles were characterized by SEM, as shown in Fig. 2. The panoramic morphology of CuO is shown in Fig. 2(a). The prepared CuO was assembled regularly from many nanosheets. The size of the entire structure is about 5 μm. Some unassembled nanosheets can be found as well. Fig. 2(b) is a high magnification of the local structure, the assembly of nanosheets can be clearly discovered. The thickness of nanosheets is about 100 nm. The panoramic morphology of Au nanoparticles is shown in Fig. 2(c). Au nanoparticles were well dispersed on the substrate with the size ranging from 50 to 200 nm. The Au nanoparticles were coated with a layer of polymer. Fig. 2(d) is a partial photomicrograph of the Au-loaded CuO. The Au nanoparticles coated by polymer attached to the CuO nanoplatelets.

3.2. Gas sensing properties

In order to research the potential applications of the Au-loaded CuO nanomaterials, pure CuO gas sensors and different concentrations of Au-loaded CuO gas sensors were fabricated. The gas sensing properties were investigated. The gas sensitivity of metal oxide semiconductors is mainly reflected by the change of material resistance[16, 20, 36]. The oxygen molecules in the air were adsorbed on the surface of CuO nanomaterial and captured electrons to form oxygen ions (O^{2-}, O^{-}, and O^{2-}). It led to the increase of holes concentration of CuO nanomaterial surface and the reduction of material resistance. When the gas sensors were exposed to the reducing organic gases, the gas molecules would react with adsorbed oxygen ions and release electrons on the surface of CuO. It would lead

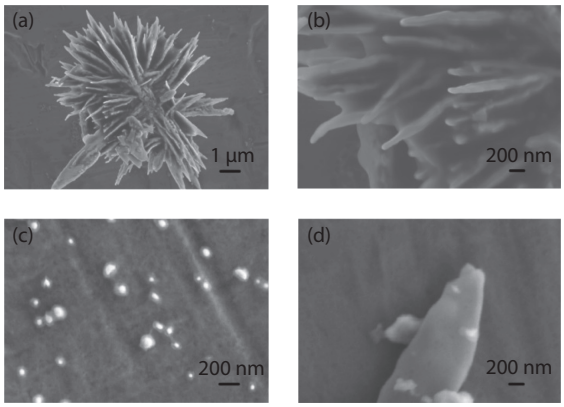

Fig. 2. SEM micrographs of (a,b) the CuO nanomaterial, (c) the Au nanoparticles, and (d) the Au-loaded CuO nanomaterial.

to the reduction of holes concentration of the CuO surface and the increase of material resistance. In general, gas sensitivity depends on the kinds of gas sensing materials, the kinds of target gases, adsorption-desorption rates, and the reaction rate of gas molecules on the surface of CuO, etc, while the performances of gas sensors depend heavily on the operating temperature, including response time, recovery time, gas response, and so on, especially the gas response[20, 37]. Therefore, the optimum operating temperature region of the gas sensor was explored. Fig. 3(a) shows the relation of gas responses with operating temperature for pure CuO, 0.5‰ Au-loaded CuO, 1.0‰ Au-loaded CuO, and 2.0‰ Au-loaded CuO gas sensors to 500 ppm of ethanol, respectively. It can be seen that pure CuO and Au-loaded CuO gas sensors both had a high response when the operating temperature was about 160 °C. The gas response of Au-loaded CuO was obviously higher than pure CuO. With the increase of operating temperature, the gas response decreased dramatically. Therefore, 160 °C was chosen as the optimum operating temperature. In general, the adsorption-desorption rate and reaction rate of gas molecules would increase with the operating temperature. It would improve the gas response. However, when the operating temperature was too high, the organic gas molecules would escape before reacting on the surface of CuO[38]. Fig. 3(b) shows the response of the sensors based on pure CuO and Au-loaded CuO to different concentrations of ethanol at 160 °C. The concentrations of ethanol were regulated from 10 to 800 ppm. It is clear that the gas response increased with the concentration of ethanol. It is noteworthy that the response of Au-loaded CuO gas sensors was significantly higher than that of pure CuO gas sensor at the same concentration, especially at high concentrations. In more detail, the response value was 4.5 (pure CuO), 7.3 (0.5 Au–CuO), 8.3 (1.0 Au–CuO), and 7.2 (2.0 Au–CuO) to 400 ppm of ethanol. With the increase of Au-loaded concentration, the response of gas sensors increased firstly and then decreased to ethanol at the same concentration. Such a phenomenon was mainly due to the catalytic effect of Au nanoparticles. However, more adsorption sites would be occupied with the increase of Au-loaded concentration. As a result, the effective surface area of CuO, which participated in adsorption-desorption reactions, and the gas response were reduced.

Figs. 4(a) and 4(b) exhibit the response and recovery behavior of the gas sensors based on pure CuO and 1.0‰ Au-loaded CuO to different concentrations of ethanol at 160 °C, re-

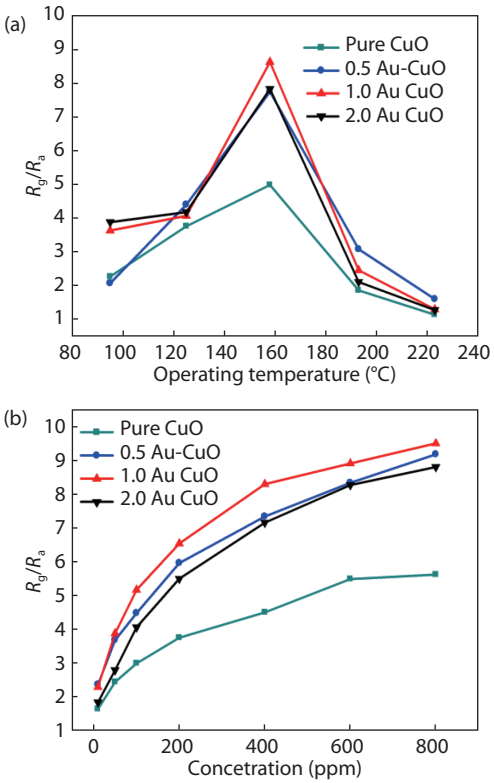

Fig. 3. (Color online) (a) Relation of the gas response with operating temperature for the pure CuO, and 0.5‰, 1.0‰, and 2.0‰ Au-loaded CuO gas sensors to 500 ppm of ethanol. (b) The response of the sensors based on pure CuO and Au-loaded CuO to different concentrations of ethanol at 160 °C.

spectively. Corresponding to Fig. 3(b), the concentrations of ethanol were regulated from 10 to 800 ppm. It can be found that the higher the ethanol concentration, the larger the gas sensors resistance in the gas. Figs. 4(c) and 4(d) exhibit the response time (T_{res}) and the recovery time (T_{rec}) of the gas sensors based on pure CuO and 1.0‰ Au-loaded CuO to 400 ppm of ethanol at 160 °C, respectively. For the pure CuO gas sensor, the response time and the recovery time was 18 and 12 s, respectively. For the 1‰ Au-loaded CuO gas sensor, the response time and the recovery time were 31 s and 32 s, respectively. Compared with the pure CuO gas sensor, the response time and the recovery time of the 1‰ Au-loaded CuO gas sensor became longer.

Note the response behavior of the pure CuO gas sensor to different concentrations of ethanol in Fig. 4. When the sensor was exposed to ethanol, the resistance increased rapidly and then decreased slightly. Subsequently, the resistance increased again. The Au-loaded CuO gas sensor also had similar behavior to a low concentration of ethanol. The prepared CuO was assembled from nanosheets. So, the nanosheets can be regarded as the basic unit, and the whole gas sensitive materials were made up by these basic units in series and parallel (ignoring the effects of grain boundary barriers). The basic unit can reflect the overall situation of gas sensitive materials. Fig. 5 shows the equivalent diagram of the resistance of Au-loaded CuO nanosheet. The equivalent resistance of the Au-loaded CuO nanosheet is R, which can also be seen as the parallel of the resistance R_1 and the resistance R_2. The R_1 is the surface resistance that mainly participated in adsorption and desorption of gases, while the R_2 is the bulk resistance away from the surface. The process of gas response could be divided into three stages. (i) Initial adsorption and reaction. When the CuO was exposed to ethanol gas, the ethanol molecules were adsorbed on the surface of the material, and a large number of holes recombined with electrons on the surface of material. It gave rise to the increase of the R_1. At this time, the concentration of the holes inside the material did not change significantly. It can be considered that the R_2 was unchanged. Therefore, the total resistance R increased. (ii) The diffusion to the surface of the holes. The rate of holes diffusion was higher than that of the electrons produced by the adsorption of ethanol. It caused the increase of the surface holes concentration and the obvious reduction of R_1. Since the change of the concentration of holes inside the CuO was very small, the R_2 had no significant increase. It eventually led to the reduction of the total resistance R. (iii) Dynamic balance of the holes. The final result was the reduction of the concentration of the total holes of CuO and the increase of the R. However, for the Au-loaded CuO gas sensors, the catalysis of gold could accelerate the rate of release of electrons in the adsorption process of ethanol. In the second stage of the response process of the Au-loaded CuO gas sensors toward the high concentration of ethanol gas, the electrons release rate was higher than the diffusion efficiency of the holes to the material surface. So, the R_1 would keep rising. As a result, it led to the continuous increase in total resistance. However, for low concentration of ethanol gas, even if there was a catalytic effect, the rate of generation of electrons would be lower than the rate of transport of the holes to the surface layer of the CuO. As a result, the total resistance R decreased in the second stage of the response process.

Selectivity is an important performance parameter of the gas sensors. Therefore, the response of gas sensors to five kinds of common organic gases with 400 ppm was researched. Fig. 6 shows the response of gas sensors (based on the pure CuO, 0.5‰ Au-loaded CuO, 1.0‰ Au-loaded CuO, and the 2.0‰ Au-loaded CuO) to 400 ppm of ethanol, methanol, acetone, formaldehyde, and xylene (C_2H_5OH, CH_3OH, CH_3COCH_3, HCHO, and C_8H_{10}) at 160 °C. The results showed that the pure CuO gas sensor had less disparity for the gas response to ethanol, methanol, acetone, and formaldehyde. Meanwhile, the response to xylene was significantly lower than the response to other gases. On the other hand, all the Au-loaded CuO gas sensors had a higher response to ethanol and xylene than the pure CuO gas sensor. It is noticed that the response of all the Au-loaded CuO gas sensors to methanol, acetone, and formaldehyde decreased compared with the pure CuO gas sensor. With the increasing of the concentration of Au nanoparticles, the decrease was more pronounced. As a result, the Au-loaded CuO gas sensors had obvious disparity for gas response to ethanol compared with other gases, especially the gas sensors based on 1.0‰ Au-loaded CuO and 2.0‰ Au-loaded CuO. It was mainly ascribed to the following two aspects. (i) Nano-gold has been widely used in physical and chemical processes as a kind of efficient catalyst. Some previous works have reported that Au can improve the gas sensing properties of metal oxide semiconductor[29, 39–42]. We considered that the Au nanoparticles can promote CuO to form more active sites on their surface in this work. These active sites can make more oxygen molecules and organic gases participate in adsorption and desorption reactions. It can increase the variation of hole concen-

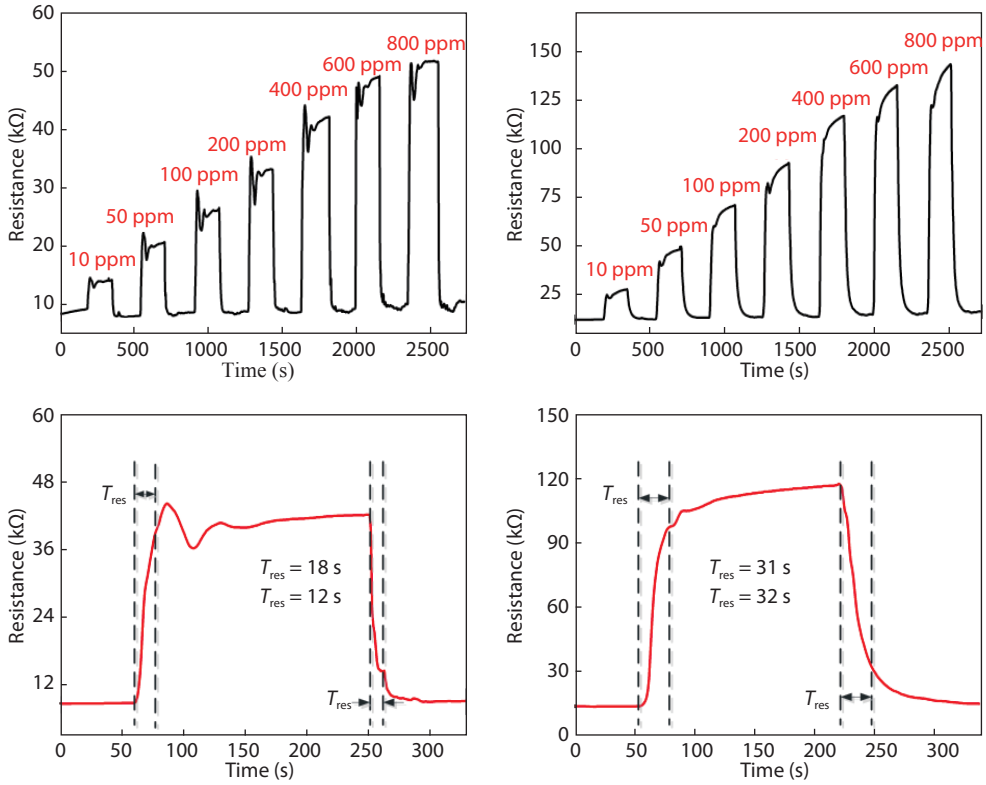

Fig. 4. (Color online) (a, b) Response and recovery behavior of the gas sensors based on pure CuO and 1.0‰ Au-loaded CuO to different concentrations of ethanol at 160 °C. (c, d) The response time (T_{res}) and the recovery time (T_{rec}) of the gas sensors based on pure CuO and 1.0‰ Au-loaded CuO to 400 ppm of ethanol at 160 °C.

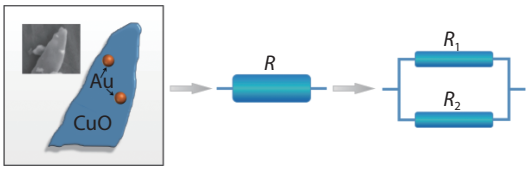

Fig. 5. (Color online) Equivalent diagram of the resistance of the Au-loaded CuO nanosheet.

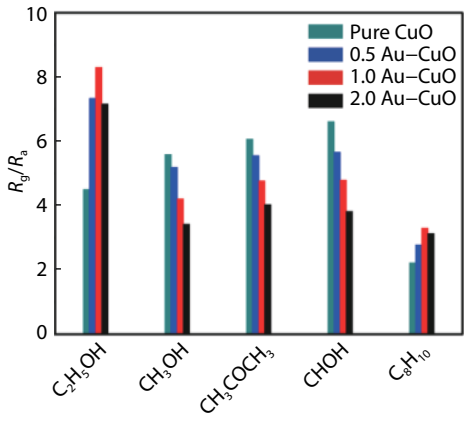

Fig. 6. (Color online) Response of the gas sensors based on the pure CuO and 0.5‰, 1.0‰, and 2.0‰ Au-loaded CuO to 400 ppm of various test gases at 160 °C.

tration of the CuO. In addition, Au nanoparticles can reduce the activation energy, which is required for the reaction of organic gases with the adsorbed oxygen of the CuO. This is the embodiment of catalytic activity of Au nanoparticles. The catalytic activity of Au nanoparticles toward ethanol was obviously higher than that of other gases in this work. Therefore, it can enhance the gas response, and result in the response of Au modified CuO to ethanol being higher than that of other gases. (ii) The residual polymer accompanied by the Au in the solution will occupy some adsorption sites on the surface of CuO. It will cause the inhibition of the gas sensing process and result in the decrease of the gas response. Considering the above factors, the response of ethanol gas was increased, while the responses of methanol, acetone, and formaldehyde were reduced. What is more, the catalytic promotion and the inhibitory effects were not obvious when the concentration of the Au was low. Therefore, it had little effect on selectivity. When the concentration of Au increased, the response of ethanol gas increased significantly, and the response of other gases decreased significantly: it would cause a significant impact on the selectivity. This phenomenon has hardly been reported, and it has great potential for improving the selectivity of gas sensors to ethanol gas. In order to compare the gas-sensing characteristics between 3D hierarchical structure CuO modified by Au nanoparticles and other typical P-type metal oxide semiconductor materials toward ethanol gas, some related reported works are listed in Table 1. It is not difficult to find out that the Au/CuO nanocomposite in our work has a lower working temperature than most of the other materials, which will help reduce the energy consumption of the device and enhance the security of measurement. Meanwhile, the higher gas response of ethanol gas provides the possibility for commercial application of the material.

Fig. 7 shows the response of the sensors based on the pure CuO and 0.5‰, 1.0‰, and 2.0‰ Au-loaded CuO to differ-

Table 1. Comparison of gas-sensing properties of other metal oxide nanostructures toward ethanol gas.

Sensing material	T (°C)	Ethanol (ppm)	Response	Reference
3D hierarchical porous structure Pt-NiO	200	500	5.0	[43]
Co_3O_4 hollow nanospheres	100	1000	6.3	[44]
MnO_2 nanorods	180	300	1.6	[45]
Comb-like Cu_2O	320	600	3.0	[46]
CuO/MWNT thin film	400	500	4.5	[47]
CuO flowers	260	1000	4.0	[20]
3D hierarchical structure Au-CuO	160	500	8.6	This work

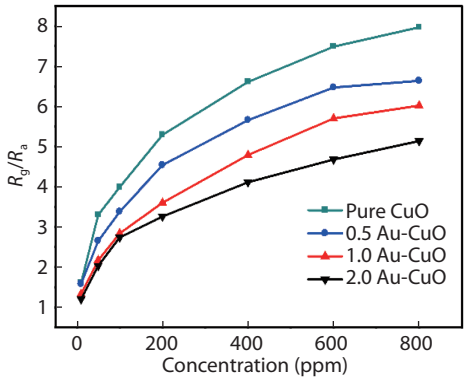

Fig. 7. (Color online) Response of the gas sensors based on the pure CuO and 0.5‰, 1.0‰, and 2.0‰ Au-loaded CuO to different concentrations of formaldehyde at 160 °C.

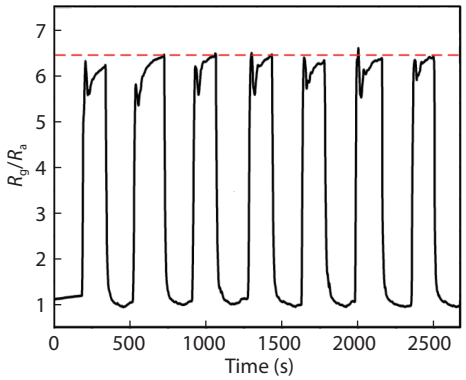

Fig. 8. (Color online) Seven cycles of response-recovery to 300 ppm of ethanol of the 2.0‰ Au-loaded CuO gas sensor at 160 °C.

ent concentrations of formaldehyde at 160 °C. The concentrations of formaldehyde were regulated from 10 to 800 ppm. The response of the Au-loaded CuO gas sensors was significantly decreased compared with the pure CuO gas sensor at the same concentration. For 400 ppm of formaldehyde, the response of the 0.5‰, 1.0‰, and 2.0‰ Au-loaded CuO gas sensors decreased to 86%, 72%, and 58% of the pure CuO gas sensor, respectively.

Stability (or repeatability) is one of the important parameters of gas sensors. Sometimes the gas sensor may have poor stability due to incomplete desorption of gas molecules and poor thermal stability of materials. So, the stability of the gas sensor was investigated by testing 300 ppm of ethanol seven times at the same conditions. Fig. 8 shows the characteristic curve of the response and recovery. There was no obvious change in response time and recovery time. It indicated that the rate of adsorption and desorption had not changed obviously. The average response was 6.4, and the variance of the response was 0.008. It shows that the Au-loaded CuO gas sensors have good stability.

4. Conclusions

In summary, the 3D nano-CuO and the Au nanoparticles were synthesized by the hydrothermal method respectively. The Au-loaded CuO gas sensors were fabricated. It is found that the Au-loaded CuO gas sensors enhanced the selectivity to ethanol by increasing the response to ethanol while reducing the response to methanol, acetone, and formaldehyde. At the optimum operating temperature of 160 °C, the response of 400 ppm of ethanol increased by 1.8 times through the load of 1.0‰ gold. It is noticed that the response of 400 ppm of methanol, acetone, and formaldehyde decreased to 61%, 66%, and 58% respectively through the load of 2.0‰ gold. Meanwhile, it is not hard to find that the Au-loaded CuO gas sensors had obvious disparity for the gas response to ethanol compared with other test gases. Furthermore, the Au-loaded CuO gas sensors had good stability. The Au nanoparticles prepared with PVP as stabilizer have great potential and promising applications in improving the selectivity of gas sensors for ethanol.

Acknowledgements

Project supported by the Provincial Natural Science Foundation of Gansu (No. 1606RJZA026), the Scientific and Technological Project of Chengguan District of Lanzhou (No. 2016-2-4), and Institute of Sensor Technology, Gansu Academy of Science.

References

[1] Gong H, Hu J Q, Wang J H, et al. Nano-crystalline Cu-doped ZnO thin film gas sensor for CO. Sensor Actuat B, 2006, 115(1), 247
[2] Zhou J, Li P, Zhang S, et al. Zeolite-modified microcantilever gas sensor for indoor air quality control. Sensor Actuat B, 2003, 94(3), 337
[3] Kawamura K, Kerman K, Fujihara M, et al. Development of a novel hand-held formaldehyde gas sensor for the rapid detection of sick building syndrome. Sensor Actuat B, 2005, 105(2), 495
[4] Tsujita W, Yoshino A, Ishida H, et al. Gas sensor network for air-pollution monitoring. Sensor Actuat B, 2005, 110(2), 304
[5] Huang H, Zhou J, Chen S, et al. A highly sensitive QCM sensor coated with Ag+-ZSM-5 film for medical diagnosis. Sensor Actuat B, 2004, 101(3), 316
[6] Abad E, Zampolli S, Marco S, et al. Flexible tag microlab development: gas sensors integration in RFID flexible tags for food logistic. Sensor Actuat B, 2007, 127(1), 2
[7] Ozawa T, Ishiguro Y, Toyoda K, et al. Detection of decomposed compounds from an early stage fire by an adsorption/combustion-type sensor. Sensor Actuat B, 2005, 108(1/2), 473

[8] Dossi N, Toniolo R, Pizzariello A, et al. An electrochemical gas sensor based on paper supported room temperature ionic liquids. Lab Chip, 2012, 12(1), 153
[9] Liu B, Yang H, Zhao H, et al. Synthesis and enhanced gas-sensing properties of ultralong NiO nanowires assembled with NiO nanocrystals. Sensor Actuat B, 2011, 156(1), 251
[10] Shen J Y, Wang M D, Wang Y F, et al. Iron and carbon codoped WO_3 with hierarchical walnut-like microstructure for highly sensitive and selective acetone sensor. Sensor Actuat B, 2018, 256, 27
[11] Li X, Zhao Y, Wang X, et al. Reduced graphene oxide (rGO) decorated TiO_2 microspheres for selective room-temperature gas sensors. Sensor Actuat B, 2016, 230, 330
[12] Tan W, Tan J, Li L, et al. Nanosheets-assembled hollowed-out hierarchical Co_3O_4 microrods for fast response/recovery gas sensor. Sensor Actuat B, 2017, 249, 66
[13] Liu C, Gao H, Wang L, et al. Facile synthesis and the enhanced sensing properties of Pt-loaded α-Fe_2O_3 porous nanospheres. Sensor Actuat B, 2017, 252, 1153
[14] Wang S, Cao J, Cui W, et al. Oxygen vacancies and grain boundaries potential barriers modulation facilitated formaldehyde gas sensing performances for In_2O_3 hierarchical architectures. Sensor Actuat B, 2018, 255, 159
[15] Khoang N D, Trung D D, Van Duy N, et al. Design of SnO_2/ZnO hierarchical nanostructures for enhanced ethanol gas-sensing performance. Sensor Actuat B, 2012, 174, 594
[16] Park H J, Choi N J, Kang H, et al. A ppb-level formaldehyde gas sensor based on CuO nanocubes prepared using a polyol process. Sensor Actuat B, 2014, 203, 282
[17] Dong C, Liu X, Xiao X, et al. Combustion synthesis of porous Pt-functionalized SnO_2 sheets for isopropanol gas detection with a significant enhancement in response. J Mater Chem A, 2014, 2(47), 20089
[18] Wang F, Li H, Yuan Z, et al. A highly sensitive gas sensor based on CuO nanoparticles synthetized via a sol-gel method. RSC Adv, 2016, 6(83), 79343
[19] Gao H, Jia H, Bierer B, et al. Scalable gas sensors fabrication to integrate metal oxide nanoparticles with well-defined shape and size. Sensor Actuat B, 2017, 249, 639
[20] Yang C, Xiao F, Wang J, et al. 3D flower- and 2D sheet-like CuO nanostructures: microwave-assisted synthesis and application in gas sensors. Sensor Actuat B, 2015, 207, 177
[21] Miller D R, Akbar S A, Morris P A. Nanoscale metal oxide-based heterojunctions for gas sensing: a review. Sensor Actuat B, 2014, 204, 250
[22] Feng C, Kou X, Chen B, et al. One-pot synthesis of In doped NiO nanofibers and their gas sensing properties. Sensor Actuat B, 2017, 253, 584
[23] Wang C, Liu J, Yang Q, et al. Ultrasensitive and low detection limit of acetone gas sensor based on W-doped NiO hierarchical nanostructure. Sensor Actuat B, 2015, 220, 59
[24] Hu X, Zhu Z, Chen C, et al. Highly sensitive H_2S gas sensors based on Pd-doped CuO nanoflowers with low operating temperature. Sensor Actuat B, 2017, 253, 809
[25] Park S, Cai Z, Lee J, et al. Fabrication of a low-concentration H_2S gas sensor using CuO nanorods decorated with Fe_2O_3 nanoparticles. Mater Lett, 2016, 181, 231
[26] Wang L, Han B, Wang Z, et al. Effective improvement of sensing performance of amperometric NO_2 sensor by Ag-modified nanostructured CuO sensing electrode. Sensor Actuat B, 2015, 207, 791
[27] Lee J S, Katoch A, Kim J H, et al. Effect of Au nanoparticle size on the gas-sensing performance of p-CuO nanowires. Sensor Actuat B, 2016, 222, 307
[28] Kim S, Park S, Park S, et al. Acetone sensing of Au and Pd-decorated WO_3 nanorod sensors. Sensor Actuat B, 2015, 209, 180
[29] Zhang S, Song P, Zhang J, et al. Highly sensitive detection of acetone using mesoporous In_2O_3 nanospheres decorated with Au nanoparticles. Sensor Actuat B, 2017, 242, 983
[30] Zhang J, Song P, Li Z, et al. Enhanced trimethylamine sensing performance of single-crystal MoO_3 nanobelts decorated with Au nanoparticles. J Alloy Compd, 2016, 685, 1024
[31] Li Z, Wang N, Lin Z, et al. Room-temperature high-performance H_2S sensor based on porous CuO nanosheets prepared by hydrothermal method. ACS Appl Mater Inter, 2016, 8(32), 20962
[32] Umar A, Alshahrani A A, Algarni H, et al. CuO nanosheets as potential scaffolds for gas sensing applications. Sensor Actuat B, 2017, 250, 24
[33] Liu X, Sun Y, Yu M, et al. Enhanced ethanol sensing properties of ultrathin ZnO nanosheets decorated with CuO nanoparticles. Sensor Actuat B, 2018, 255, 3384
[34] Sun X M, Li Y D. Ag@C core/shell structured nanoparticles: controlled synthesis, characterization, and assembly. Langmuir, 2005, 21(13), 6019
[35] Yang H, Liu Z H. Preparation and properties of flower-like CuO nanostructures. J Shaanxi Normal University, 2009, 37(6), 60
[36] Liu X, Chen N, Han B, et al. Nanoparticle cluster gas sensor: Pt activated SnO_2 nanoparticles for NH_3 detection with ultrahigh sensitivity. Nanoscale, 2015, 7(36), 14872
[37] Bai S, Liu X, Li D, et al. Synthesis of ZnO nanorods and its application in NO_2 sensors. Sensor Actuat B, 2011, 153(1), 110
[38] Guo G S, Lin K W, Han D M, et al. Functionalization of flower-like ZnO nanostructures with Au@CuO nanoparticles for detection of ethanol. IEEE Sens J, 2014, 14(6), 1797
[39] Li X, Feng W, Xiao Y, et al. Hollow zinc oxide microspheres functionalized by Au nanoparticles for gas sensors. RSC Adv, 2014, 4(53), 28005
[40] Li X, Zhou X, Guo H, et al. Design of Au@ZnO yolk-shell nanospheres with enhanced gas sensing properties. ACS Appl Mater Inter, 2014, 6(21), 18661
[41] Wang L, Wang S, Xu M, et al. A Au-functionalized ZnO nanowire gas sensor for detection of benzene and toluene. Phys Chem Chem Phys, 2013, 15(40), 17179
[42] Guo J, Zhang J, Zhu M, et al. High-performance gas sensor based on ZnO nanowires functionalized by Au nanoparticles. Sensor Actuat B, 2014, 199, 339
[43] Dong C, Li Q, Chen G, et al. Enhanced formaldehyde sensing performance of 3D hierarchical porous structure Pt-functionalized NiO via a facile solution combustion synthesis. Sensor Actuat B, 2015, 220, 171
[44] Park J, Shen X, Wang G. Solvothermal synthesis and gas-sensing performance of Co_3O_4 hollow nanospheres. Sensor Actuat B, 2009, 136(2), 494
[45] Liu C, Navale ST, Yang ZB, et al. Ethanol gas sensing properties of hydrothermally grown α-MnO_2 nanorods. J Alloy Compd, 2017, 727, 362
[46] Guan L, Pang H, Wang J, et al. Fabrication of novel comb-like Cu_2O nanorod-based structures through an interface etching method and their application as ethanol sensors. Chem Commun, 2010, 46(37), 7022
[47] Parmar M, Bhatia R, Prasad V, et al. Ethanol sensing using CuO/MWNT thin film. Sensor Actuat B, 2011, 158(1), 229